

CHAPTER

4

LINEAR WIRE ANTENNAS

4.1 INTRODUCTION

Wire antennas, linear or curved, are some of the oldest, simplest, cheapest, and in many cases the most versatile for many applications. It should not then come as a surprise to the reader that we begin our analysis of antennas by considering some of the oldest, simplest, and most basic configurations. Initially we will try to minimize the complexity of the antenna structure and geometry to keep the mathematical details to a minimum.

4.2 INFINITESIMAL DIPOLE

An infinitesimal linear wire ($l \ll \lambda$) is positioned symmetrically at the origin of the coordinate system and oriented along the z axis, as shown in Figure 4.1(a). Although infinitesimal dipoles are not very practical, they are used to represent capacitor-plate (also referred to as *top-hat-loaded*) antennas. In addition, they are utilized as building blocks of more complex geometries. The wire, in addition to being very small ($l \ll \lambda$), is very thin ($a \ll \lambda$). The current is assumed to be constant and given by

$$\mathbf{I}(z') = \hat{\mathbf{a}}_z I_0 \quad (4-1)$$

where $I_0 = \text{constant}$.

4.2.1 Radiated Fields

To find the fields radiated by the current element, the two-step procedure of Figure 3.1 is used. It will be required to determine first \mathbf{A} and \mathbf{F} and then find the \mathbf{E} and \mathbf{H} . The functional relation between \mathbf{A} and the source \mathbf{J} is given by (3-49), (3-51), or (3-53). Similar relations are available for \mathbf{F} and \mathbf{M} , as given by (3-50), (3-52), and (3-54).

Since the source only carries an electric current \mathbf{I}_e , \mathbf{I}_m and the potential function \mathbf{F} are zero. To find \mathbf{A} we write

$$\mathbf{A}(x, y, z) = \frac{\mu}{4\pi} \int_C \mathbf{I}_e(x', y', z') \frac{e^{-jkR}}{R} dl' \quad (4-2)$$

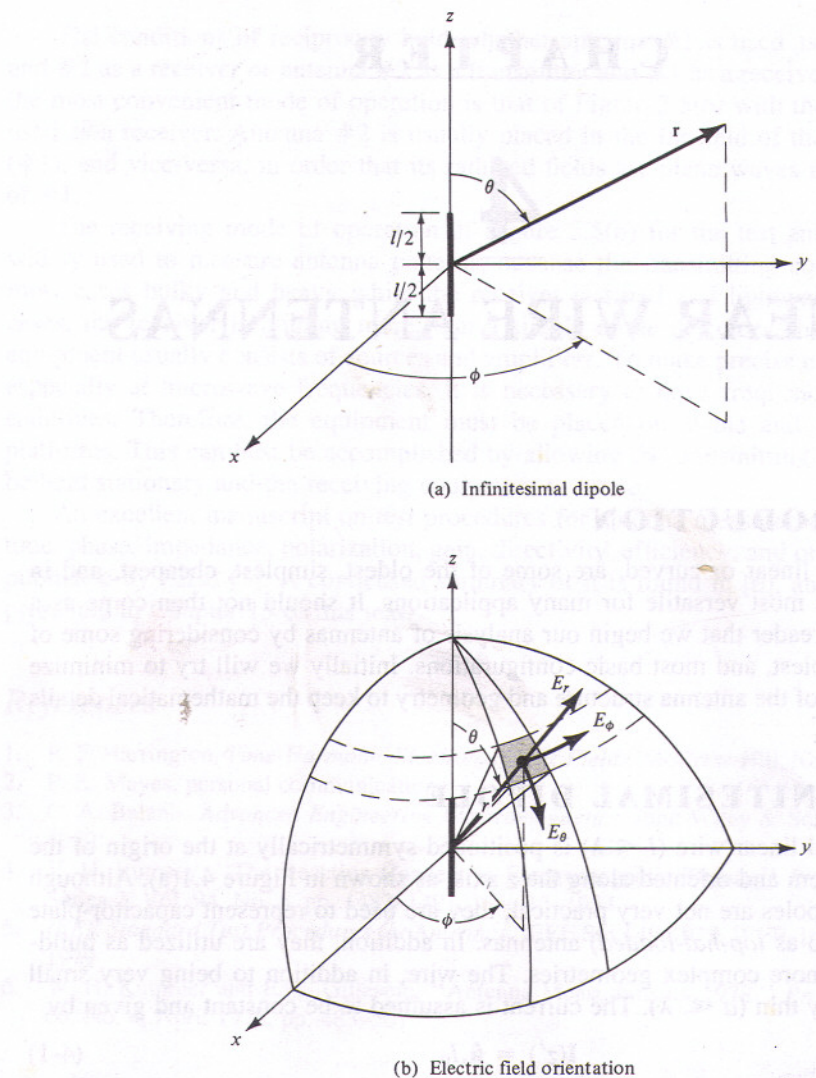


Figure 4.1 Geometrical arrangement of an infinitesimal dipole and its associated electric field components on a spherical surface.

where (x, y, z) represent the observation point coordinates, (x', y', z') represent the coordinates of the source, R is the distance from any point on the source to the observation point, and path C is along the length of the source. For the problem of Figure 4.1

$$\mathbf{I}_e(x', y', z') = \hat{\mathbf{a}}_z I_0 \quad (4-3a)$$

$$x' = y' = z' = 0 \quad (\text{infinitesimal dipole}) \quad (4-3b)$$

$$R = \sqrt{(x - x')^2 + (y - y')^2 + (z - z')^2} = \sqrt{x^2 + y^2 + z^2} \quad (4-3c)$$

$$= r = \text{constant} \quad (4-3c)$$

$$dl' = dz' \quad (4-3d)$$

we can write (4-2) as

$$\mathbf{A}(x, y, z) = \hat{\mathbf{a}}_z \frac{\mu I_0}{4\pi r} e^{-jkr} \int_{-l/2}^{+l/2} dz' = \hat{\mathbf{a}}_z \frac{\mu I_0 l}{4\pi r} e^{-jkr} \quad (4-4)$$

The next step of the procedure is to find \mathbf{H}_A using (3-2a) and then \mathbf{E}_A using (3-15) or (3-10) with $\mathbf{J} = 0$. To do this, it is often much simpler to transform (4-4) from rectangular to spherical components and then use (3-2a) and (3-15) or (3-10) in spherical coordinates to find \mathbf{H} and \mathbf{E} .

The transformation between rectangular and spherical components is given, in matrix form, by (see Appendix VII)

$$\begin{bmatrix} A_r \\ A_\theta \\ A_\phi \end{bmatrix} = \begin{bmatrix} \sin \theta \cos \phi & \sin \theta \sin \phi & \cos \theta \\ \cos \theta \cos \phi & \cos \theta \sin \phi & -\sin \theta \\ -\sin \phi & \cos \phi & 0 \end{bmatrix} \begin{bmatrix} A_x \\ A_y \\ A_z \end{bmatrix} \quad (4-5)$$

For this problem, $A_x = A_y = 0$, so (4-5) reduces to

$$A_r = A_z \cos \theta = \frac{\mu I_0 l e^{-jkr}}{4\pi r} \cos \theta \quad (4-6a)$$

$$A_\theta = -A_z \sin \theta = -\frac{\mu I_0 l e^{-jkr}}{4\pi r} \sin \theta \quad (4-6b)$$

$$A_\phi = 0 \quad (4-6c)$$

Using the symmetry of the problem (no variations in ϕ), (3-2a) can be expanded in spherical coordinates and written in simplified form as

$$\mathbf{H} = \hat{\mathbf{a}}_\phi \frac{1}{\mu r} \left[\frac{\partial}{\partial r} (r A_\theta) - \frac{\partial A_r}{\partial \theta} \right] \quad (4-7)$$

Substituting (4-6a)–(4-6c) into (4-7) reduces it to

$$H_r = H_\theta = 0 \quad (4-8a)$$

$$H_\phi = j \frac{k I_0 l \sin \theta}{4\pi r} \left[1 + \frac{1}{jkr} \right] e^{-jkr} \quad (4-8b)$$

The electric field \mathbf{E} can now be found using (3-15) or (3-10) with $\mathbf{J} = 0$. That

$$\mathbf{E} = \mathbf{E}_A = -j\omega \mathbf{A} - j \frac{1}{\omega \mu \epsilon} \nabla (\nabla \cdot \mathbf{A}) = \frac{1}{j\omega \epsilon} \nabla \times \mathbf{H} \quad (4-9)$$

Substituting (4-6a)–(4-6c) or (4-8a)–(4-8b) into (4-9) reduces it to

$$E_r = \eta \frac{I_0 l \cos \theta}{2\pi r^2} \left[1 + \frac{1}{jkr} \right] e^{-jkr} \quad (4-10a)$$

$$E_\theta = j\eta \frac{k I_0 l \sin \theta}{4\pi r} \left[1 + \frac{1}{jkr} - \frac{1}{(kr)^2} \right] e^{-jkr} \quad (4-10b)$$

$$E_\phi = 0 \quad (4-10c)$$

The **E**- and **H**-field components are valid everywhere, except on the source itself, and they are sketched in Figure 4.1(b) on the surface of a sphere of radius r . It is a straightforward exercise to verify Equations (4-10a)–(4-10c), and this is left as an exercise to the reader (Prob. 4.9).

4.2.2 Power Density and Radiation Resistance

The input impedance of an antenna, which consists of real and imaginary parts, was discussed in Section 2.13. For a lossless antenna, the real part of the input impedance was designated as radiation resistance. It is through the mechanism of the radiation resistance that power is transferred from the guided wave to the free-space wave. To find the input resistance for a lossless antenna, the Poynting vector is formed in terms of the **E**- and **H**-fields radiated by the antenna. By integrating the Poynting vector over a closed surface (usually a sphere of constant radius), the total power radiated by the source is found. The real part of it is related to the input resistance.

For the infinitesimal dipole, the complex Poynting vector can be written using (4-8a)–(4-8b) and (4-10a)–(4-10c) as

$$\begin{aligned}\mathbf{W} &= \frac{1}{2}(\mathbf{E} \times \mathbf{H}^*) = \frac{1}{2}(\hat{\mathbf{a}}_r E_r + \hat{\mathbf{a}}_\theta E_\theta) \times (\hat{\mathbf{a}}_\phi H_\phi^*) \\ &= \frac{1}{2}(\hat{\mathbf{a}}_r E_\theta H_\phi^* - \hat{\mathbf{a}}_\theta E_r H_\phi^*)\end{aligned}\quad (4-11)$$

whose radial W_r and transverse W_θ components are given, respectively, by

$$W_r = \frac{\eta}{8} \left| \frac{I_0 l}{\lambda} \right|^2 \frac{\sin^2 \theta}{r^2} \left[1 - j \frac{1}{(kr)^3} \right] \quad (4-12a)$$

$$W_\theta = j\eta \frac{k|I_0 l|^2 \cos \theta \sin \theta}{16\pi^2 r^3} \left[1 + \frac{1}{(kr)^2} \right] \quad (4-12b)$$

The complex power moving in the radial direction is obtained by integrating (4-11)–(4-12b) over a closed sphere of radius r . Thus it can be written as

$$P = \oint_S \mathbf{W} \cdot d\mathbf{s} = \int_0^{2\pi} \int_0^\pi (\hat{\mathbf{a}}_r W_r + \hat{\mathbf{a}}_\theta W_\theta) \cdot \hat{\mathbf{a}}_r r^2 \sin \theta d\theta d\phi \quad (4-13)$$

which reduces to

$$P = \int_0^{2\pi} \int_0^\pi W_r r^2 \sin \theta d\theta d\phi = \eta \frac{\pi}{3} \left| \frac{I_0 l}{\lambda} \right|^2 \left[1 - j \frac{1}{(kr)^3} \right] \quad (4-14)$$

The transverse component W_θ of the power density does not contribute to the integral. Thus (4-14) does not represent the total complex power radiated by the antenna. Since W_θ , as given by (4-12b), is purely imaginary, it will not contribute to any real radiated power. However, it does contribute to the imaginary (reactive) power which along with the second term of (4-14) can be used to determine the total reactive power of the antenna. The reactive power density, which is most dominant for small values of kr , has both radial and transverse components. It merely changes between outward and inward directions to form a standing wave at a rate of twice per cycle. It also moves in the transverse direction as suggested by (4-12b).

Equation (4-13), which gives the real and imaginary power that is moving outwardly, can also be written as [4]

$$\begin{aligned} P &= \frac{1}{2} \iint_S \mathbf{E} \times \mathbf{H}^* \cdot d\mathbf{s} = \eta \left(\frac{\pi}{3} \right) \left| \frac{I_0 l}{\lambda} \right|^2 \left[1 - j \frac{1}{(kr)^3} \right] \\ &= P_{\text{rad}} + j2\omega(\tilde{W}_m - \tilde{W}_e) \end{aligned} \quad (4-15)$$

where

P = power (in radial direction)

P_{rad} = time-average power radiated

\tilde{W}_m = time-average magnetic energy density (in radial direction)

\tilde{W}_e = time-average electric energy density (in radial direction)

$2\omega(\tilde{W}_m - \tilde{W}_e)$ = time-average imaginary (reactive) power (in radial direction)

From (4-14)

$$P_{\text{rad}} = \eta \left(\frac{\pi}{3} \right) \left| \frac{I_0 l}{\lambda} \right|^2 \quad (4-16)$$

and

$$2\omega(\tilde{W}_m - \tilde{W}_e) = -\eta \left(\frac{\pi}{3} \right) \left| \frac{I_0 l}{\lambda} \right|^2 \frac{1}{(kr)^3} \quad (4-17)$$

It is clear from (4-17) that the radial electric energy must be larger than the radial magnetic energy. For large values of kr ($kr \gg 1$ or $r \gg \lambda$), the reactive power diminishes and vanishes when $kr = \infty$.

Since the antenna radiates its real power through the radiation resistance, for the infinitesimal dipole it is found by equating (4-16) to

$$P_{\text{rad}} = \eta \left(\frac{\pi}{3} \right) \left| \frac{I_0 l}{\lambda} \right|^2 = \frac{1}{2} |I_0|^2 R_r \quad (4-18)$$

where R_r is the radiation resistance. Equation (4-18) reduces to

$$R_r = \eta \left(\frac{2\pi}{3} \right) \left(\frac{l}{\lambda} \right)^2 = 80\pi^2 \left(\frac{l}{\lambda} \right)^2 \quad (4-19)$$

for a free-space medium ($\eta \approx 120\pi$). It should be pointed out that the radiation resistance of (4-19) represents the total radiation resistance since (4-12b) does not contribute to it.

For a wire antenna to be classified as an infinitesimal dipole, its overall length must be very small (usually $l \leq \lambda/50$).

Example 4.1

Find the radiation resistance of an infinitesimal dipole whose overall length is $l = \lambda/50$.

SOLUTION

Using (4-19)

$$R_r = 80\pi^2 \left(\frac{l}{\lambda}\right)^2 = 80\pi^2 \left(\frac{1}{50}\right)^2 = 0.316 \text{ ohms}$$

Since the radiation resistance of an infinitesimal dipole is about 0.3 ohms, it will present a very large mismatch when connected to practical transmission lines, many of which have characteristic impedances of 50 or 75 ohms. The reflection efficiency (ϵ_r) and hence the overall efficiency (ϵ_t) will be very small.

The reactance of an infinitesimal dipole is capacitive. This can be illustrated by considering the dipole as a flared open-circuited transmission line, as discussed in Section 1.4. Since the input impedance of an open-circuited transmission line a distance $l/2$ from its open end is given by $Z_{in} = -jZ_c \cot(\beta l/2)$, where Z_c is the characteristic impedance, it will always be negative (capacitive) for $l \ll \lambda$.

4.2.3 Radian Distance and Radian Sphere

The E- and H-fields for the infinitesimal dipole, as represented by (4-8a)–(4-8b) and (4-10a)–(4-10c), are valid everywhere (except on the source itself). An inspection of these equations reveals the following:

- (a) At a distance $r = \lambda/2\pi$ (or $kr = 1$), which is referred to as the *radian distance*, the magnitude of the first and second terms within the brackets of (4-8b) and (4-10a) is the same. Also at the radian distance the magnitude of all three terms within the brackets of (4-10b) is identical; the only term that contributes to the total field is the second, because the first and third terms cancel each other. This is illustrated in Figure 4.2.
- (b) At distances less than the radian distance $r < \lambda/2\pi$ ($kr < 1$), the magnitude of the second term within the brackets of (4-8b) and (4-10a) is greater than the first term and begins to dominate as $r \ll \lambda/2\pi$. For (4-10b) and $r < \lambda/2\pi$, the magnitude of the third term within the brackets is greater than the magnitude of the first and second terms while the magnitude of the second term is greater than that of the first one; each of these terms begins to dominate as $r \ll \lambda/2\pi$. This is illustrated in Figure 4.2. The region $r < \lambda/2\pi$ ($kr < 1$) is referred to as the *near-field region*.
- (c) At distances greater than the radian distance $r > \lambda/2\pi$ ($kr > 1$), the first term within the brackets of (4-8b) and (4-10a) is greater than the magnitude of the second term and begins to dominate as $r \gg \lambda/2\pi$ ($kr \gg 1$). For (4-10b) and $r > \lambda/2\pi$, the first term within the brackets is greater than the magnitude of the second and third terms while the magnitude of the second term is greater than that of the third; each of these terms begins to dominate as $r \gg \lambda/2\pi$. This is illustrated in Figure 4.2. The region $r > \lambda/2\pi$ ($kr > 1$) is referred to as the *intermediate-field region* while that for $r \gg \lambda/2\pi$ ($kr \gg 1$) is referred to as the *far-field region*.

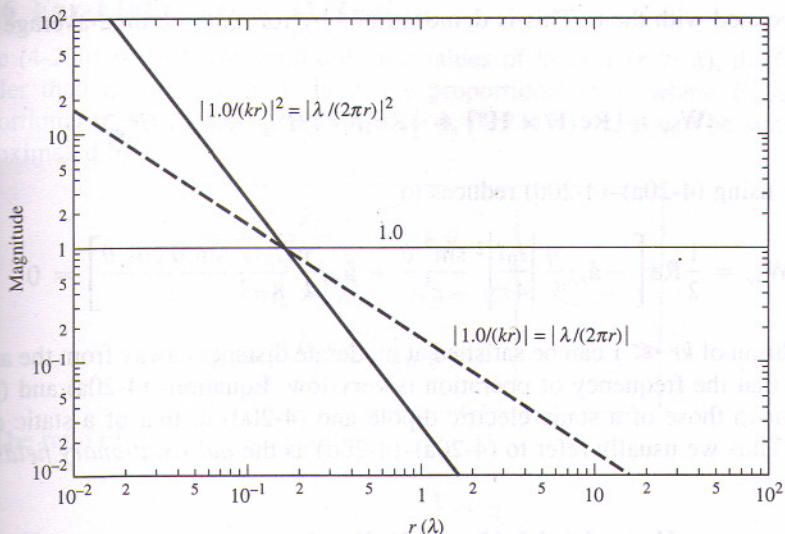


Figure 4.2 Magnitude variation, as a function of the radial distance, of the field terms radiated by an infinitesimal dipole.

- (1) The sphere with radius equal to the radian distance ($r = \lambda/2\pi$) is referred as the *radian sphere*, and it defines the region within which the reactive power density is greater than the radiated power density [1]–[3]. For an antenna, the radian sphere represents the volume occupied mainly by the stored energy of the antenna's electric and magnetic fields. Outside the radian sphere the radiated power density is greater than the reactive power density and begins to dominate as $r \gg \lambda/2\pi$. Therefore the radian sphere can be used as a reference, and it defines the transition between stored energy pulsating primarily in the θ direction [represented by (4-12b)] and energy radiating in the radial (r) direction [represented by the first term of (4-12a); the second term represents stored energy pulsating in the radial (r) direction].

4.2.4 Near-Field ($kr \ll 1$) Region

An inspection of (4-8a)–(4-8b) and (4-10a)–(4-10c) reveals that for $kr \ll \lambda$ or $r \ll \lambda/2\pi$ they can be reduced in much simpler form and can be approximated by

$$\left. \begin{aligned} E_r &\approx -j\eta \frac{I_0 l e^{-jkr}}{2\pi k r^3} \cos \theta \\ E_\theta &\approx -j\eta \frac{I_0 l e^{-jkr}}{4\pi k r^3} \sin \theta \end{aligned} \right\} kr \ll 1 \quad (4-20a)$$

$$E_\phi = H_r = H_\theta = 0 \quad (4-20b)$$

$$H_\phi \approx \frac{I_0 l e^{-jkr}}{4\pi r^2} \sin \theta \quad (4-20c)$$

The E-field components, E_r and E_θ , are in time-phase but they are in time phase quadrature with the H-field component H_ϕ ; therefore there is no time-average power

flow associated with them. This is demonstrated by forming the time-average power density as

$$\mathbf{W}_{av} = \frac{1}{2} \operatorname{Re}[\mathbf{E} \times \mathbf{H}^*] = \frac{1}{2} \operatorname{Re}[\hat{\mathbf{a}}_r E_\theta H_\phi^* - \hat{\mathbf{a}}_\theta E_r H_\phi^*] \quad (4-21)$$

which by using (4-20a)–(4-20d) reduces to

$$\mathbf{W}_{av} = \frac{1}{2} \operatorname{Re} \left[-\hat{\mathbf{a}}_r j \frac{\eta}{k} \left| \frac{I_0 l}{4\pi} \right|^2 \frac{\sin^2 \theta}{r^5} + \hat{\mathbf{a}}_\theta j \frac{\eta}{k} \frac{|I_0 l|^2}{8\pi^2} \frac{\sin \theta \cos \theta}{r^5} \right] = 0 \quad (4-22)$$

The condition of $kr \ll 1$ can be satisfied at moderate distances away from the antenna provided that the frequency of operation is very low. Equations (4-20a) and (4-20b) are similar to those of a static electric dipole and (4-20d) to that of a static current element. Thus we usually refer to (4-20a)–(4-20d) as the *quasistationary fields*.

4.2.5 Intermediate-Field ($kr > 1$) Region

As the values of kr begin to increase and become greater than unity, the terms that were dominant for $kr \ll 1$ become smaller and eventually vanish. For moderate values of kr the \mathbf{E} -field components lose their in-phase condition and approach time-phase quadrature. Since their magnitude is not the same, in general, they form a rotating vector whose extremity traces an ellipse. This is analogous to the polarization problem except that the vector rotates in a plane parallel to the direction of propagation and is usually referred to as the *cross field*. At these intermediate values of kr , the E_θ and H_ϕ components approach time-phase, which is an indication of the formation of time-average power flow in the outward (radial) direction (radiation phenomenon).

As the values of kr become moderate ($kr > 1$), the field expressions can be approximated again but in a different form. In contrast to the region where $kr \ll 1$, the first term within the brackets in (4-8b) and (4-10a) becomes more dominant and the second term can be neglected. The same is true for (4-10b) where the second and third terms become less dominant than the first. Thus we can write for $kr > 1$

$$E_r = \eta \frac{I_0 l e^{-jkr}}{2\pi r^2} \cos \theta \quad (4-23a)$$

$$E_\theta \approx j\eta \frac{k I_0 l e^{-jkr}}{4\pi r} \sin \theta \quad kr > 1 \quad (4-23b)$$

$$E_\phi = H_r = H_\theta = 0 \quad (4-23c)$$

$$H_\phi \approx j \frac{k I_0 l e^{-jkr}}{4\pi r} \sin \theta \quad (4-23d)$$

The total electric field is given by

$$\mathbf{E} = \hat{\mathbf{a}}_r E_r + \hat{\mathbf{a}}_\theta E_\theta \quad (4-24)$$

whose magnitude can be written as

$$|\mathbf{E}| = \sqrt{|E_r|^2 + |E_\theta|^2} \quad (4-25)$$

4.2.6 Far-Field ($kr \gg 1$) Region

Since (4-23a)–(4-23d) are valid only for values of $kr > 1$ ($r > \lambda$), then E_r will be smaller than E_θ because E_r is inversely proportional to r^2 where E_θ is inversely proportional to r . In a region where $kr \gg 1$, (4-23a)–(4-23d) can be simplified and approximated by

$$\left. \begin{aligned} E_\theta &\approx j\eta \frac{kI_0 le^{-jkr}}{4\pi r} \sin \theta \\ E_r &\approx E_\phi = H_r = H_\theta = 0 \end{aligned} \right\} kr \gg 1 \quad (4-26a)$$

$$E_r \approx E_\phi = H_r = H_\theta = 0 \quad (4-26b)$$

$$\left. \begin{aligned} H_\phi &\approx j \frac{kI_0 le^{-jkr}}{4\pi r} \sin \theta \end{aligned} \right\} kr \gg 1 \quad (4-26c)$$

The ratio of E_θ to H_ϕ is equal to

$$Z_w = \frac{E_\theta}{H_\phi} \approx \eta \quad (4-27)$$

where

Z_w = wave impedance

η = intrinsic impedance ($377 \approx 120\pi$ ohms for free-space)

The \mathbf{E} - and \mathbf{H} -field components are perpendicular to each other, transverse to the radial direction of propagation, and the r variations are separable from those of θ and ϕ . The shape of the pattern is not a function of the radial distance r , and the fields form a Transverse ElectroMagnetic (TEM) wave whose wave impedance is equal to the intrinsic impedance of the medium. As it will become even more evident in later chapters, this relationship is applicable in the far-field region of all antennas of finite dimensions. Equations (4-26a)–(4-26c) can also be derived using the procedure outlined and relationships developed in Section 3.6. This is left as an exercise to the reader (Prob. 4.11).

Example 4.2

For an infinitesimal dipole determine and interpret the vector effective length. At what incidence angle does the open-circuit maximum voltage occurs at the output terminals of the dipole if the electric field intensity of the incident wave is 10 mvolts/meter? The length of the dipole is 10 cm.

SOLUTION

Using (4-26a) and the effective length as defined by (2-92), we can write that

$$\begin{aligned} \mathbf{E} &= \hat{\mathbf{a}}_\theta j\eta \frac{kI_0 le^{-jkr}}{4\pi r} \sin \theta = -\hat{\mathbf{a}}_\theta j\eta \frac{kI_0 e^{-jkr}}{4\pi r} \cdot (-\hat{\mathbf{a}}_\theta l \sin \theta) \\ &= -\hat{\mathbf{a}}_\theta j\eta \frac{kI_0 e^{-jkr}}{4\pi r} \cdot \ell_e \end{aligned}$$

Therefore, the effective length is

$$\ell_e = -\hat{\mathbf{a}}_\theta l \sin \theta$$

whose maximum value occurs when $\theta = 90^\circ$, and it is equal to l . Therefore, to achieve maximum output the wave must be incident upon the dipole at a normal incidence angle ($\theta = 90^\circ$).

The open-circuit maximum voltage is equal to

$$\begin{aligned} V_{oc} \Big|_{\max} &= |\mathbf{E}^i \cdot \ell_e|_{\max} = |\hat{\mathbf{a}}_\theta 10 \times 10^{-3} \cdot (-\hat{\mathbf{a}}_\theta l \sin \theta)|_{\max} \\ &= 10 \times 10^{-3} l = 10^{-3} \text{ volts} \end{aligned}$$

4.2.7 Directivity

The real power P_{rad} radiated by the dipole was found in Section 4.2.2, as given by (4-16). The same expression can be obtained by first forming the average power density, using (4-26a)–(4-26c). That is,

$$\mathbf{W}_{av} = \frac{1}{2} \operatorname{Re}(\mathbf{E} \times \mathbf{H}^*) = \hat{\mathbf{a}}_r \frac{1}{2\eta} |E_\theta|^2 = \hat{\mathbf{a}}_r \frac{\eta}{2} \left| \frac{k I_0 l}{4\pi} \right|^2 \frac{\sin^2 \theta}{r^2} \quad (4-28)$$

Integrating (4-28) over a closed sphere of radius r reduces it to (4-16). This is left as an exercise to the reader (Prob. 4.10).

Associated with the average power density of (4-28) is a radiation intensity U which is given by

$$U = r^2 W_{av} = \frac{\eta}{2} \left(\frac{k I_0 l}{4\pi} \right)^2 \sin^2 \theta = \frac{r^2}{2\eta} |E_\theta(r, \theta, \phi)|^2 \quad (4-29)$$

and it conforms with (2-12a). The normalized pattern of (4-29) is shown in Figure 4.3. The maximum value occurs at $\theta = \pi/2$ and it is equal to

$$U_{\max} = \frac{\eta}{2} \left(\frac{k I_0 l}{4\pi} \right)^2 \quad (4-30)$$

Using (4-16) and (4-30), the directivity reduces to

$$D_0 = 4\pi \frac{U_{\max}}{P_{rad}} = \frac{3}{2} \quad (4-31)$$

and the maximum effective aperture to

$$A_{em} = \left(\frac{\lambda^2}{4\pi} \right) D_0 = \frac{3\lambda^2}{8\pi} \quad (4-32)$$

The radiation resistance of the dipole can be obtained by the definition of (4-18). Since the radiated power obtained by integrating (4-28) over a closed sphere is the same as that of (4-16), the radiation resistance using it will also be the same as obtained previously and given by (4-19).

Integrating the complex Poynting vector over a closed sphere, as was done in (4-13), results in the power (real and imaginary) directed in the radial direction. Any

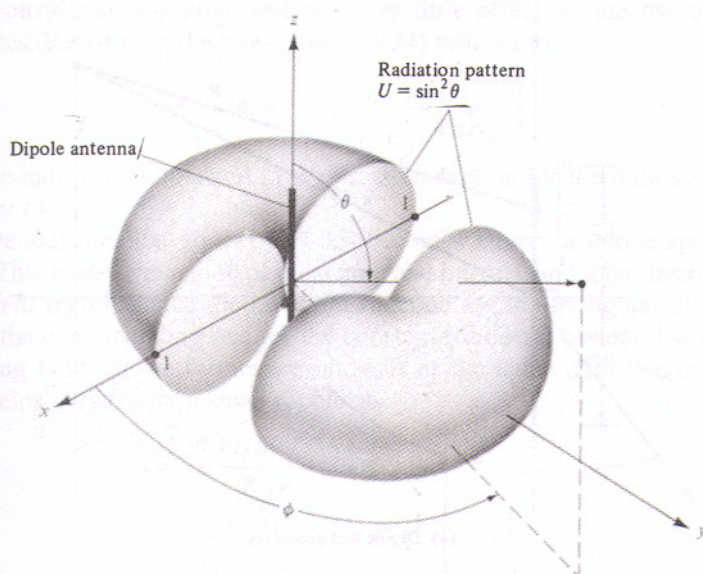


Figure 4.3 Three-dimensional radiation pattern of infinitesimal dipole.

transverse components of power density, as given by (4-12b), will not be captured by the integration even though they are part of the overall power. Because of this limitation, this method cannot be used to derive the input reactance of the antenna.

4.3 SMALL DIPOLE

The creation of the current distribution on a thin wire was discussed in Section 1.4, and it was illustrated with some examples in Figure 1.16. The radiation properties of an infinitesimal dipole, which is usually taken to have a length $l \leq \lambda/50$, were discussed in the previous section. Its current distribution was assumed to be constant. Although a constant current distribution is not realizable (other than top-hat-loaded elements), it is a mathematical quantity that is used to represent actual current distributions of antennas that have been incremented into many small lengths.

A better approximation of the current distribution of wire antennas, whose lengths are usually $\lambda/50 < l \leq \lambda/10$, is the triangular variation of Figure 1.16(a). The sinusoidal variations of Figures 1.16(b)–(c) are more accurate representations of the current distribution of any length wire antenna.

The most convenient geometrical arrangement for the analysis of a dipole is usually to have it positioned symmetrically about the origin with its length directed along the z -axis, as shown in Figure 4.4(a). This is not necessary, but it is usually the most convenient. The current distribution of a small dipole ($\lambda/50 < l \leq \lambda/10$) is shown in Figure 4.4(b), and it is given by

$$\mathbf{I}_e(x', y', z') = \begin{cases} \hat{\mathbf{a}}_z I_0 \left(1 - \frac{2}{l} z'\right), & 0 \leq z' \leq l/2 \\ \hat{\mathbf{a}}_z I_0 \left(1 + \frac{2}{l} z'\right), & -l/2 \leq z' \leq 0 \end{cases} \quad (4-33)$$

where $I_0 = \text{constant}$.

numerical solution, and it is shown in Figure 8.13(b) where it is compared with the ideal distribution of (4-56) and other available data. For the moment method solution, a gap at the feed has been inserted. As expected and illustrated in Figure 8.13(b), the current distribution for the $l = \lambda/2$ dipole based on (4-56) is not that different from that based on the moment method. This is also illustrated by (4-82). Therefore the input resistance based on these two methods will not be that different. However, for the $l = \lambda$ dipole, the current distribution based on (4-56) is quite different, especially at and near the feed point, compared to that based on the moment method, as shown in Figure 8.13(b). This is expected since the current distribution based on the ideal current distribution is zero at the feed point; for practical antennas it is very small. Therefore the gap at the feed plays an important role on the current distribution at and near the feed point. In turn, the values of the input resistance based on the two methods will be quite different, since there is a significant difference in the current between the two methods. This is discussed further in Chapter 8.

4.6 HALF-WAVELENGTH DIPOLE

One of the most commonly used antennas is the half-wavelength ($l = \lambda/2$) dipole. Because its radiation resistance is 73 ohms, which is very near the 75-ohm characteristic impedance of some transmission lines, its matching to the line is simplified especially at resonance. Because of its wide acceptance in practice, we will examine in a little more detail its radiation characteristics.

The electric and magnetic field components of a half-wavelength dipole can be obtained from (4-62a) and (4-62b) by letting $l = \lambda/2$. Doing this, they reduce to

$$(4-84) \quad E_\theta \approx j\eta \frac{I_0 e^{-jkr}}{2\pi r} \left[\frac{\cos\left(\frac{\pi}{2} \cos \theta\right)}{\sin \theta} \right]$$

$$(4-85) \quad H_\phi \approx j \frac{I_0 e^{-jkr}}{2\pi r} \left[\frac{\cos\left(\frac{\pi}{2} \cos \theta\right)}{\sin \theta} \right]$$

In turn, the time-average power density and radiation intensity can be written, respectively, as

$$(4-86) \quad W_{av} = \eta \frac{|I_0|^2}{8\pi^2 r^2} \left[\frac{\cos\left(\frac{\pi}{2} \cos \theta\right)}{\sin \theta} \right]^2 \simeq \eta \frac{|I_0|^2}{8\pi^2 r^2} \sin^3 \theta$$

and

$$(4-87) \quad U = r^2 W_{av} = \eta \frac{|I_0|^2}{8\pi^2} \left[\frac{\cos\left(\frac{\pi}{2} \cos \theta\right)}{\sin \theta} \right]^2 \simeq \eta \frac{|I_0|^2}{8\pi^2} \sin^3 \theta$$

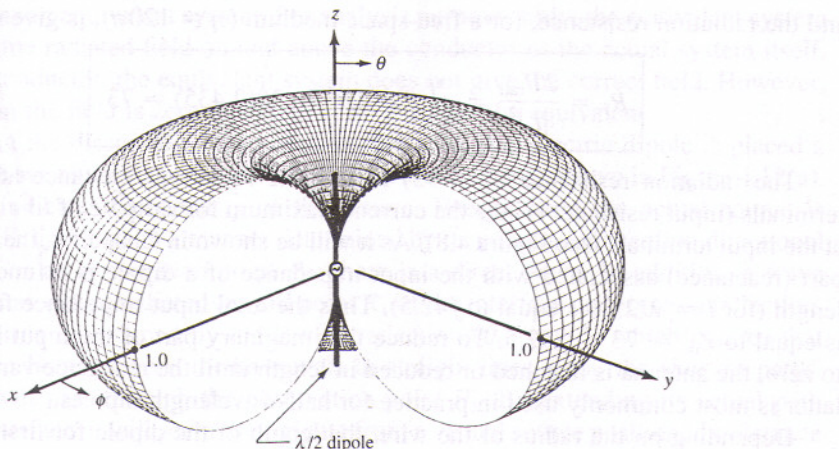


Figure 4.11 Three-dimensional pattern of a $\lambda/2$ dipole.

(SOURCE: C. A. Balanis, "Antenna Theory: A Review" Proc. IEEE, Vol. 80, No 1. Jan. 1992. © 1992 IEEE.)

whose two-dimensional pattern is shown plotted in Figure 4.6 while the three-dimensional pattern is depicted in Figure 4.11. For the three-dimensional pattern of Figure 4.11, a 90° angular sector has been removed to illustrate the figure-eight elevation plane pattern variations.

The total power radiated can be obtained as a special case of (4-67), or

$$P_{\text{rad}} = \eta \frac{|I_0|^2}{4\pi} \int_0^{\pi} \frac{\cos^2\left(\frac{\pi}{2} \cos \theta\right)}{\sin \theta} d\theta \quad (4-88)$$

which when integrated reduces, as a special case of (4-68), to

$$P_{\text{rad}} = \eta \frac{|I_0|^2}{8\pi} \int_0^{2\pi} \left(\frac{1 - \cos y}{y} \right) dy = \eta \frac{|I_0|^2}{8\pi} C_{\text{in}}(2\pi) \quad (4-89)$$

By the definition of $C_{\text{in}}(x)$, as given by (4-69), $C_{\text{in}}(2\pi)$ is equal to

$$C_{\text{in}}(2\pi) = 0.5772 + \ln(2\pi) - C_i(2\pi) = 0.5772 + 1.838 - (-0.02) \approx 2.435 \quad (4-90)$$

where $C_i(2\pi)$ is obtained from the tables in Appendix III.

Using (4-87), (4-89), and (4-90), the directivity of the half-wavelength dipole reduces to

$$D_0 = 4\pi \frac{U_{\max}}{P_{\text{rad}}} = 4\pi \frac{U|_{\theta=\pi/2}}{P_{\text{rad}}} = \frac{4}{C_{\text{in}}(2\pi)} = \frac{4}{2.435} \approx 1.643 \quad (4-91)$$

The corresponding maximum effective area is equal to

$$A_{\text{em}} = \frac{\lambda^2}{4\pi} D_0 = \frac{\lambda^2}{4\pi} (1.643) \approx 0.13\lambda^2 \quad (4-92)$$